ACCSCIENCE PUBLISHING

Asian Journal of Water, Environment and Pollution

ORIGINAL RESEARCH ARTICLE

Transcriptomic and proteomic profiling of antibiotic resistance gene expression in bacteria exposed to uranium stress

Shuai Zhou[1], Xiulan Ou[1], Jian Song[2], Yi Duan[1], Shuang Li[1], Zidong Yang[1], Yuyu Li[1], Anqi Chen[1], Shuying Li[3], Yuanyuan Gao[1]*, and Chengyun Zhou[3,4]*

[1]Hunan Province Key Laboratory of Pollution Control and Resources Reuse Technology, School of Civil Engineering, University of South China, Hengyang, Hunan, China

[2]Hunan Province Key Laboratory of Rare Metal Minerals Exploitation and Geological Disposal of Wastes, School of Resources, Environment and Safety Engineering, University of South China, Hengyang, Hunan, China

[3]Key Laboratory of Monitoring for Heavy Metal Pollutants, Ministry of Ecology and Environment, Changsha, Hunan, China

[4]Key Laboratory of Environmental Biology and Pollution Control, College of Environmental Science and Engineering, Hunan University, Changsha, Hunan, China

***Corresponding authors:**
Yuanyuan Gao
(GaoYuanyuan@usc.edu.cn);
Chengyun Zhou
(zhouchengyun@hnu.edu.cn)

Citation: Zhou S, Ou X, Song J, *et al*. Transcriptomic and proteomic profiling of antibiotic resistance gene expression in bacteria exposed to uranium stress. *Asian J Water Environ Pollut*. 2026;23(3):026050025.
doi: 10.36922/AJWEP026050025

Received: January 28, 2026

Revised: February 24, 2026

Accepted: March 9, 2026

Published online: May 4, 2026

Abstract

Uranium (U) exerts combined chemical and radiological toxicity to bacteria, yet its regulatory impact on the expression of antibiotic resistance genes (ARGs) remains poorly understood. In this study, we profiled the transcriptomic and proteomic responses of Gram-negative *Escherichia coli* and Gram-positive *Bacillus subtilis* under exposure to U at environmentally relevant concentrations. At 0.05 and 5 mg/L U, *E. coli* exhibited 6 (4 up, 2 down) and 80 (29 up, 51 down) differentially expressed genes (DEGs), respectively, while *B. subtilis* showed 566 (193 up, 373 down) and 432 (125 up, 307 down) DEGs. Each bacterium adopted distinct strategies for modulating the expression of ARGs, including those encoding efflux pumps. *E. coli* coordinately upregulated toxin–antitoxin modules, quorum-sensing machinery, and two-component systems, shifting to a tolerance state. Conversely, *B. subtilis* repressed these systems transcriptionally while reinforcing cell wall-associated two-component pathways at the protein level, thereby maintaining active growth and repair. Together, our findings reveal the molecular mechanisms through which radioactive heavy metals may promote the evolution of antibiotic resistance, providing a framework for assessing resistance risks in U-contaminated environments.

Keywords: Uranium; Antibiotic resistance genes; *Escherichia coli*; *Bacillus subtilis*; Transcriptomics; Proteomics

1. Introduction

The spread of antibiotic resistance genes (ARGs) in the environment can be accelerated by exogenous chemical pollutants such as heavy metals and pharmaceuticals.[1,2] These contaminants can also significantly increase the transcription of ARGs, particularly

those encoding efflux pumps, thereby promoting the evolution of multidrug resistance.[3] For example, long-term exposure to copper (Cu) induces significant upregulation of genes associated with the AcrAB–TolC multidrug efflux pump (e.g., *acrB* and *marR*) in *Escherichia coli*.[4] Similarly, chromium (Cr) stress markedly increases the mRNA levels of ARGs such as *mepA* and *norA* in *Staphylococcus aureus* by up to several tenfold.[5] Transcriptomic analysis of multidrug-resistant *E. coli* further showed that Cr elevated expression of efflux pump genes (*bcr*, *mdtG*, and *mdtL*) and the polymyxin resistance gene *arnA* by 1.5- to 29.2-fold.[6] Such transcriptional responses have been reported to raise the minimum inhibitory concentration of antibiotics by 4–8-fold and enhance plasmid transfer frequency by 2.3-fold.[7,8] Collectively, heavy metals may activate ARG expression at the transcriptional level, thereby accelerating the evolution of drug-resistant phenotypes.

Unlike non-radioactive metals, uranium (U) imposes not only chemical toxicity but also radiolysis.[9] This combined effect undermines membrane integrity and may consequently alter ARGs' abundance and mobility. ARGs are frequently co-detected with U in mining areas and receiving rivers, with a significant positive correlation between them ($p < 0.05$).[10] Metagenomic data have indicated that 5 mg/L U increased the total relative abundance of intracellular and extracellular ARGs in activated sludge by 1.8-fold,[11] an effect exceeding that of equivalent concentrations of Cu or Cr.[12] Additionally, in U-contaminated soils, multidrug resistance determinants, such as *mexF* and *tnpA*, showed a direct positive correlation with U concentration, implying that U may select for antibiotic resistance.[13] While most studies have catalogued the presence and diversity of ARGs, the dynamic expression of these genes under U stress remains largely unexplored.[14] This knowledge gap hinders a mechanistic understanding of bacterial adaptive evolution and the true origins of resistance in radioactive environments. Our recent work has found that U exposure upregulated genes involved in DNA uptake and homologous recombination, thereby promoting the horizontal transfer of ARGs.[15] Nevertheless, the molecular circuitry that links U stress to ARG expression and transfer remains unresolved.

To bridge this gap, we combined transcriptomics and proteomics to quantify ARG expression and regulation in two model organisms exposed to environmentally relevant U concentrations. The Gram-negative *Escherichia coli* and the Gram-positive *Bacillus subtilis* were chosen because they are ubiquitous in nature and have served as benchmark strains for studying metal–antibiotic cross-resistance.[16] In addition, they are routinely recovered from U mining sites and have been shown to tolerate moderate U loads.[17] Our objectives were: (i) to characterize the distinct molecular adaptations of *E. coli* and *B. subtilis* to U stress using integrated transcriptomics and proteomics, and (ii) to elucidate how the activation of specific pathways, including efflux pumps and toxin–antitoxin (TA) systems, contributes to the evolution of multidrug resistance. The findings provide a mechanistic framework for evaluating the risks of antibiotic resistance in environments contaminated with radioactive heavy metals.

2. Materials and methods

2.1. Culture conditions and uranium exposure experiments

Gram-negative *E. coli* and Gram-positive *B. subtilis* were selected as model organisms. Both strains, purchased from the China General Microbiological Culture Collection Center, are commonly found in U-contaminated sites in China and display moderate U tolerance and adaptive capacity.[16-18] Single colonies of *E. coli* and *B. subtilis* were taken from freshly streaked Luria–Bertani (LB) agar plates and incubated in LB medium overnight at 37 °C with shaking at 150 rpm. The LB medium was adjusted to pH 7.0 ± 0.2 using 1 M hydrochloric acid or sodium hydroxide prior to sterilization. U was introduced into the medium as uranyl nitrate hexahydrate, which dissociates to form the stable uranyl ion (UO_2^{2+}) at neutral pH. These cultures were then diluted into fresh LB medium supplemented with 0, 0.05, or 5 mg/L U, based on environmentally relevant concentrations reported in surface water and groundwater.[15,18,19] Growth was monitored by measuring the optical density (OD_{600}) hourly for 24 h (BioTek, USA), using sterile medium as a blank. Three biological replicates were prepared for each strain and treatment. Growth curves were fitted with a logistic model to obtain maximum specific growth rates and lag phase duration.

For U exposure tests, an independent pre-culture grown to early exponential phase ($OD_{600} \approx 0.2$) was used to inoculate (1 % v/v) into 500 mL LB medium containing the targeted concentration of U. Cultures were incubated at 37 °C and 180 rpm, and 25 mL aliquots were harvested at three hours (late lag phase) and eight hours (mid-exponential phase). The two time points were chosen based on strain growth dynamics and stress-induced expression patterns. The three-hour mark represents the late lag phase, when transcriptional responses to stress peak.[20] The eight-hour mark falls in mid-exponential phase, when protein-level changes are most active.[21] Cells were pelleted at 8,000 × g for five minutes at 4 °C, washed twice with ice-cold phosphate-buffered saline, snap frozen in liquid nitrogen,

and stored at −80 °C until RNA or protein extraction.

2.2. RNA extraction and sequencing

Total RNA was extracted with the E.Z.N.A. Soil RNA Midi Kit (Omega Bio-tek, United States) following the manufacturer's instructions. Ribosomal RNA was removed with the RiboCop Mixed Bacterial rRNA Depletion Kit (Lexogen, Austria). RNA integrity was verified on a 2,100 Bioanalyzer (RNA integrity number ≥ 8; Agilent, USA). Sequencing libraries were prepared from RNA using the NEBNext Ultra II Directional RNA Library Prep Kit (New England Biolabs, United States), which included fragmentation, first- and second-strand cDNA synthesis, end-repair, A-tailing, adapter ligation, and a 12-cycle polymerase chain reaction enrichment. Libraries were quantified by Qubit and quantitative polymerase chain reaction, pooled in equimolar amounts, and sequenced on an Illumina NovaSeq X Plus platform (2 × 150 bp paired-end). Raw reads were processed by adapter trimming with Cutadapt (version 3.8) and quality filtering (Phred score ≥ 30, length ≥ 25 nt) to yield clean reads, which were then aligned to the respective reference genomes (*E. coli* K-12 MG1655, GCF_000005845.2; *B. subtilis* 168, GCF_000009045.1) using Bowtie2 (version 2.5.4) in very sensitive local mode.

2.3. Protein extraction and proteomic analysis

Frozen cell pellets were thawed on ice and resuspended in lysis buffer. Cells were lysed through a combination of vortexing, mechanical grinding, and three cycles of indirect sonication (180 s per cycle). The lysate was then centrifuged at 14,000 × g for 15 min at 4 °C, and the supernatant was collected for protein quantification using the bicinchoninic acid assay. For each sample, 100 μg of protein was reduced, alkylated, and desalted by acetone precipitation. The precipitated protein was resuspended in digestion buffer and digested with trypsin at 37 °C for 16 h. The resulting peptides were desalted on C18 StageTips and reconstituted in 0.1% (v/v) formic acid. Peptide separation was performed on a reversed-phase column using a Vanquish Neo ultra-high-performance liquid chromatography system (Thermo Fisher Scientific, United States). Mass spectrometry analysis was conducted in positive-ion mode on an Orbitrap Astral mass spectrometer (Thermo Fisher Scientific, United States) using data-independent acquisition (DIA). To support DIA data processing, a spectral library was constructed from complementary data-dependent acquisition runs, which were processed with Proteome Discoverer (version 2.1; ThermoFisher Scientific, United States). The DIA data were then analyzed in Spectronaut (version 18; Biognosys, Switzerland) using the spectral library for peptide matching, peak extraction, and label-free quantification to obtain protein identifications and abundances.

2.4. Transcriptomic and proteomic data analysis

Transcript abundances were quantified with RSEM (v1.3.3) and reported as transcripts per million. Differential gene expression analysis was conducted with DESeq2 (version 1.30.0). For transcriptomic analysis, statistical significance for differentially expressed genes was defined as $|\log_2$ fold change (LFC)$| \geq 1$ with an adjusted p-value < 0.05 (Benjamini–Hochberg correction). For proteomic analysis, differentially expressed proteins were defined as those with $|\log_2$ fold change$| \geq 1$ and $p < 0.05$, along with an FDR (q-value) < 0.05. Benjamini–Hochberg correction was indeed applied in the proteomic data analysis, with a q-value < 0.05 used as the filtering criterion. All proteins reported as differentially expressed satisfied the $q < 0.05$ threshold.

Functional enrichment analysis of Gene Ontology (GO) and Kyoto Encyclopedia of Genes and Genomes (KEGG) pathways was carried out using clusterProfiler. Genes and proteins annotated to TA systems or quorum sensing (QS) were selected, with priority given to those exhibiting the largest LFC among significant hits. Fold changes of transcript and protein were visualized in corresponding heatmaps generated with the pheatmap package in R (version 4.3), and the correlation between omic layers was evaluated using Spearman's rank correlation coefficient. For genes with matched transcriptomic and proteomic data, Spearman's rank correlation coefficients were calculated between mRNA levels and DIA intensities, and significance was assessed using permutation tests ($p < 0.05$). Gene–protein pairs exhibiting opposite directional changes and $|\text{LFC}| \geq 1$ in both datasets were defined as significantly discordant and subsequently subjected to KEGG pathway enrichment analysis.

2.5. Statistical analysis

All transcriptomic and proteomic analyses were performed with three independent biological replicates. Data are presented as mean ± standard deviation. Pairwise comparisons were conducted with two-tailed independent-samples t-tests in the Statistical Package for Social Sciences (version 26), with $p < 0.05$ considered statistically significant. All plots were prepared using Origin 2023 and R (version 4.3).

3. Results and discussion

3.1. Cell viability under environmentally relevant uranium stress

To assess the impact of U on bacterial growth, both strains

were exposed to 0, 0.05, or 5 mg/L U. Growth curve analysis showed no significant inhibition in either species at 0.05 or 5 mg/L U ($p > 0.05$; Figure 1A and 1B), confirming their ability to proliferate normally under environmentally relevant U stress. Such low-to-moderate U levels are generally non-toxic to indigenous microbial communities.[18] *E. coli* and *B. subtilis* are established indigenous strains in U-contaminated environments,[17] with well-documented U tolerance from previous isolation studies.[22] Both organisms exhibited typical growth phases, i.e., lag (0–4 h), log (4–14 h), and stationary (>14 h) phases, with highly consistent growth patterns. Transcriptional remodeling was most pronounced during the early lag phase, while translational changes peaked in the mid-exponential phase. Therefore, cells were harvested at three and eight hours, respectively, for subsequent transcriptomic and proteomic analyses.[20,21]

3.2. Transcriptional responses of bacteria to uranium stress

To elucidate how *E. coli* and *B. subtilis* respond transcriptionally to U stress, a comparative transcriptomic analysis was performed. In *E. coli,* 0.05 mg/L U yielded 6 differentially expressed genes (DEGs) (4 up, 2 down), whereas 5 mg/L U produced 80 DEGs (29 up, 51 down) (Figure 2A and 2B). In contrast, *B. subtilis* displayed markedly greater transcriptional changes, with 566 DEGs (193 up, 373 down) at 0.05 mg/L U and 432 DEGs (125 up, 307 down) at 5 mg/L U (Figure 2C and 2D). These results indicate that *B. subtilis* exhibits a more sensitive transcriptional response than *E. coli.*

To assess the functional implications of these transcriptional changes, GO enrichment analysis was performed, which classifies gene functions into molecular function, biological process, and cellular component categories.[23] In *E. coli*, 16 and 214 GO terms were significantly enriched at 0.05 and 5 mg/L U, respectively (Figure S1A & B). Under 5 mg/L U stress, GO cellular-component terms such as cytoplasm, plasma membrane, and integral component of membrane were overrepresented (Figure S1B). This pattern aligns with the known role of envelope-associated proteins in U detoxification[22] and supports the view that maintaining envelope integrity is critical for U tolerance in *E. coli*. In *B. subtilis*, 27 and 24 GO terms were enriched at the two respective doses, including dominant clusters related to catalytic activity, response to stimulus, transporter activity, and cellular anatomical entity (Figure S1C & D). The enrichment of transporter activity suggests that this strain counteracts U stress by increasing import/export capacity and activating general stress-response networks.

The KEGG pathway mapping further revealed metabolic divergence between the two species. At 0.05 mg/L U, only the two-component system (TCS) was enriched in *E. coli* (Figure 2E). In contrast, 5 mg/L U additionally activated QS, butanoate metabolism, fatty acid degradation, and geraniol degradation, with fatty acid degradation being the most prominent (Figure 2F). In *B. subtilis*, a broader pathway response was observed, with 122 and 98 pathways enriched at 0.05 and 5 mg/L U, respectively (Figure 2G and 2H). Specifically, adenosine triphosphate-binding cassette (ABC) transporters, aminoacyl tRNA biosynthesis, QS, and TCSs were significantly enriched. This profile is consistent with previous reports indicating that *Bacillus spp*. upregulate amino acid metabolism and transport to mitigate metal-induced oxidative and proteotoxic stress.[24] Collectively, the pathway profiles show species-specific adaptation strategies, in which *E. coli* primarily relies on membrane lipid remodeling and fatty acid turnover,

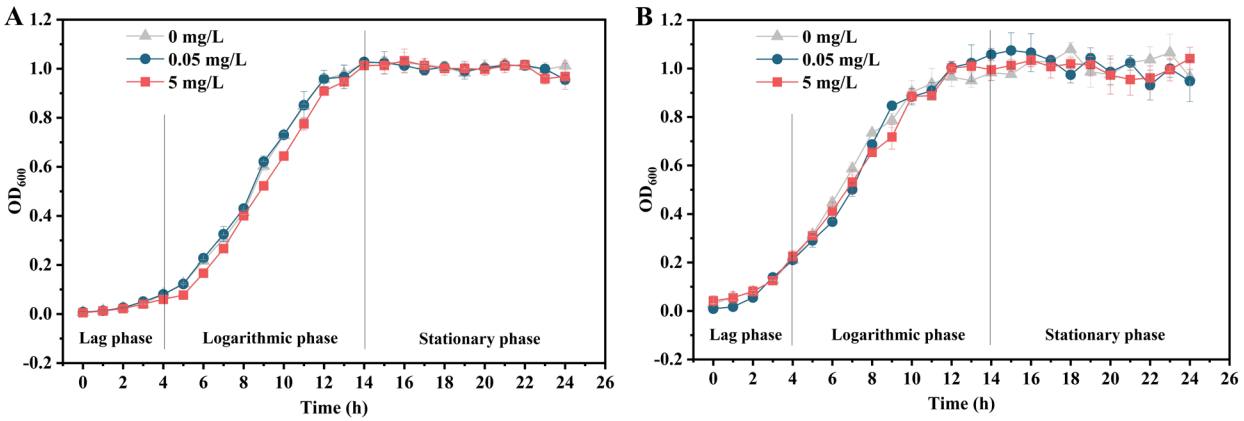

Figure 1. Growth curves of bacteria under uranium stress. (A) *Escherichia coli.* (B) *Bacillus subtilis.*

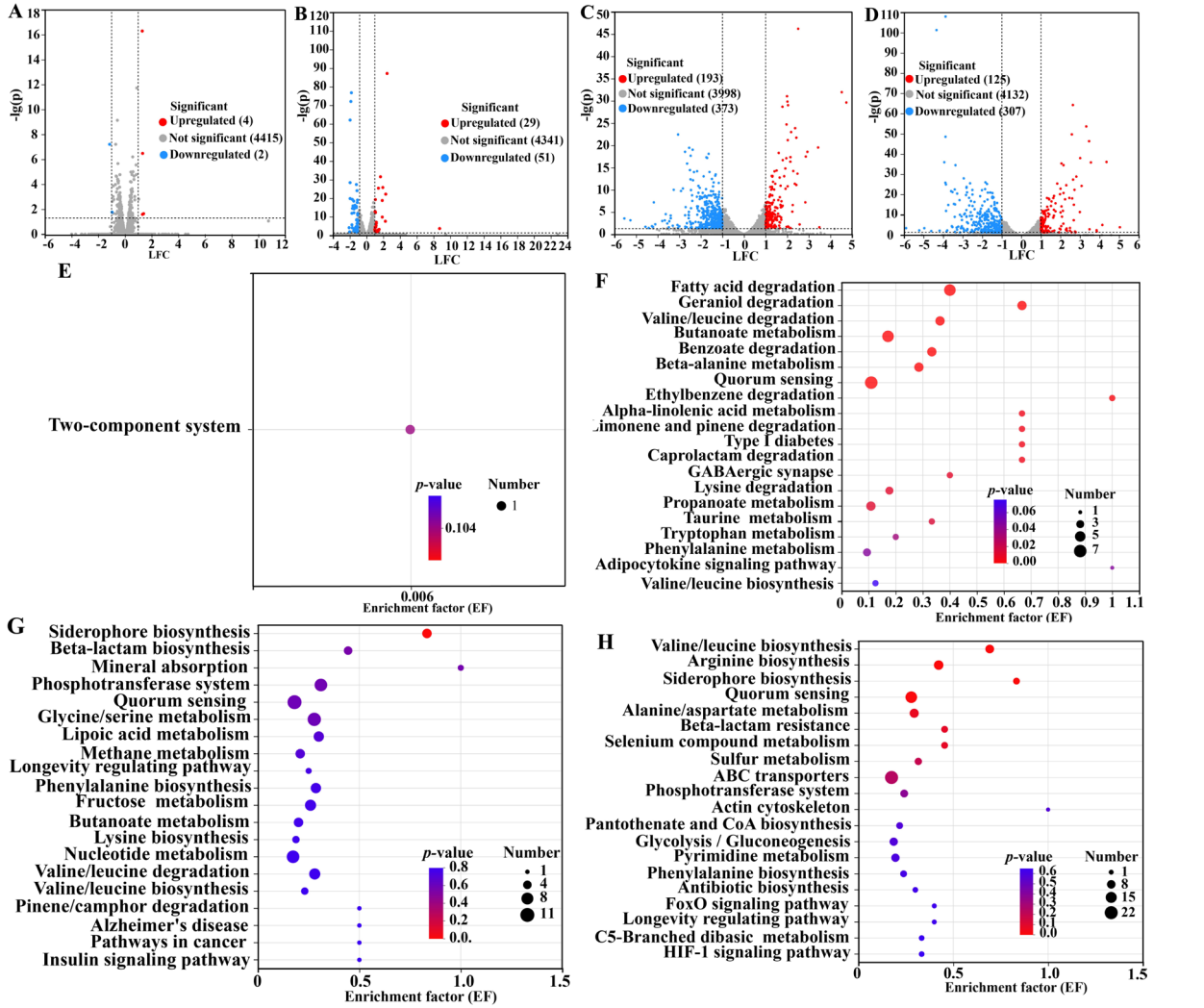

Figure 2. Comparative transcriptomic analysis under uranium (U) stress. (A–D) Volcano plots showing differentially expressed genes in *Escherichia coli* and *Bacillus subtilis* under different U concentrations. Red and blue dots denote significantly upregulated ($\log_2$ fold change [LFC] ≥ 1, adjusted $p < 0.05$) and downregulated (LFC ≤ –1, adjusted $p < 0.05$) differentially expressed genes (DEGs), respectively; grey dots represent non-DEGs. The number of DEGs is indicated next to the corresponding color in the legend. (A) *E. coli* at 0.05 mg/L U. (B) *E. coli* at 5 mg/L U. (C) *B. subtilis* at 0.05 mg/L U. (D) *B. subtilis* at 5 mg/L U. (E–H) Kyoto Encyclopedia of Genes and Genomes pathway enrichment analysis of DEGs. Bubble size reflects gene count per pathway, and color intensity indicates statistical significance, with darker hues corresponding to smaller *p*-values. (E) *E. coli* at 0.05 mg/L U. (F) *E. coli* at 5 mg/L U. (G) *B. subtilis* at 0.05 mg/L U. (H) *B. subtilis* at 5 mg/L U. All data are derived from three biological replicates.

whereas *B. subtilis* prioritizes amino acid biosynthesis and efflux transport. *E. coli* possesses an outer membrane composed of lipopolysaccharide and a thin peptidoglycan layer, rendering its cell envelope more susceptible to U's chemical and radiotoxicity. It thus depends on membrane lipid remodeling for damage repair.[25] In contrast, *B. subtilis* features a thick, peptidoglycan-rich cell wall and lacks an outer membrane, conferring greater structural robustness. This bacterium modulates intracellular U accumulation via specific metal uptake systems and preferentially activates amino acid biosynthesis and efflux pathways to alleviate U-induced stress.[26]

3.3. Proteomic responses of bacteria to uranium stress

Further quantitative proteomic analysis corroborated the transcriptomic trends. In *E. coli*, 89 proteins (39 up, 50 down) and 98 proteins (36 up, 62 down) showed differential abundance at 0.05 and 5 mg/L U, respectively (Figure 3A and 3B). *B. subtilis* again displayed a broader response, with 84 proteins (29 up, 55 down) at 0.05 mg/L U and 1,180 proteins (461 up, 719 down) at 5 mg/L U (Figure 3C and

3D). These data indicate that U stress markedly perturbs proteostasis in both species, with a more pronounced effect at a higher U concentration. This finding is consistent with proteomic studies of other U-tolerant bacteria, which have demonstrated dose-dependent changes in protein expression under U stress.[27,28]

The GO enrichment analysis identified 18 and 20 significantly enriched terms in *E. coli* at the two U doses, with binding, catalytic activity, cellular process, and metabolic process as the dominant categories (Figure S2A & B). In *B. subtilis*, 17 and 26 terms were enriched, highlighting catalytic activity, cellular process, and anatomical entity (Figure S2C & D). The recurring enrichment of catalytic activity across both species suggests an increased investment in enzymes that accelerate central carbon and nitrogen flux, facilitating rapid metabolic adaptation under U stress.[29]

The KEGG pathway analysis further provided insights

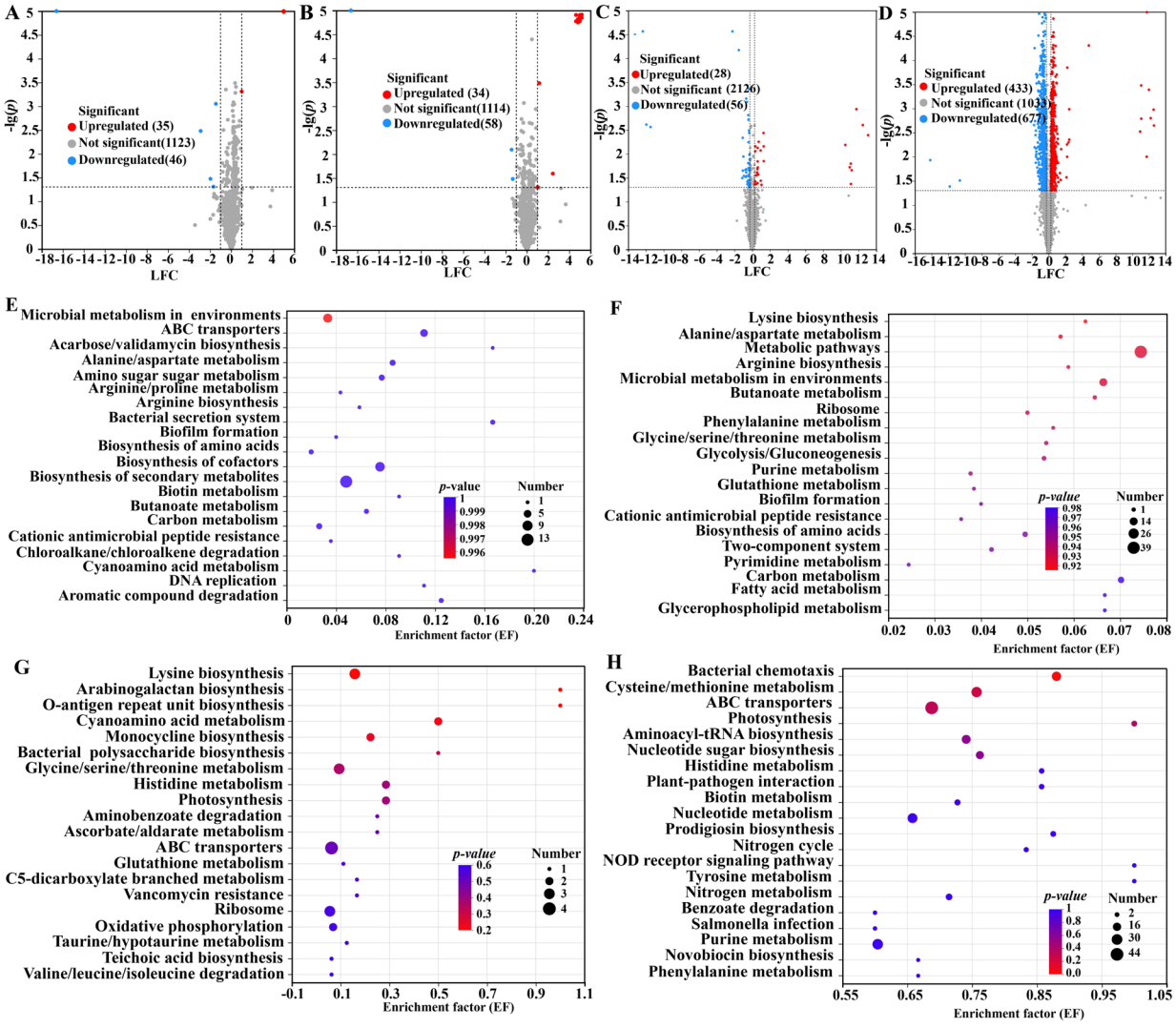

Figure 3. Comparative proteomic profiling of bacteria under uranium (U) stress. (A–D) Volcano plots showing differentially abundant proteins (DAPs) in *Escherichia coli* and *Bacillus subtilis* under different U concentrations. Red and blue dots denote significantly upregulated ($\log_2$ fold change [LFC] ≥ 1, $p < 0.05$) and downregulated (LFC ≤ –1, $p < 0.05$) DAPs, respectively; gray dots indicate proteins without significant differential expression. The number of DAPs is indicated next to the corresponding color in the legend. (A) *E. coli* at 0.05 mg/L U. (B) *E. coli* at 5 mg/L U. (C) *B. subtilis* at 0.05 mg/L U. (D) *B. subtilis* at 5 mg/L U. (E–H) Kyoto Encyclopedia of Genes and Genomes pathway enrichment analysis of DAPs. Bubble size reflects gene count per pathway, and color intensity indicates statistical significance, with darker hues corresponding to smaller *p*-values. (E) *E. coli* at 0.05 mg/L U. (F) *E. coli* at 5 mg/L U. (G) *B. subtilis* at 0.05 mg/L U. (H) *B. subtilis* at 5 mg/L U. All data are derived from three biological replicates.

into the metabolic strategies adopted by each species. In *E. coli,* 65 and 69 pathways were significantly enriched at 0.05 and 5 mg/L U, respectively, with metabolic pathways and biosynthesis of secondary metabolites forming the largest categories (Figure 3E and 3F). This global metabolic shift indicates a systemic reallocation of cellular resources to maintain homeostasis under U stress.[30] By contrast, *B. subtilis* exhibited 40 and 123 enriched pathways under the same conditions. At 0.05 mg/L U, ABC transporters and lysine biosynthesis were most prominent, whereas 5 mg/L U further enriched TCSs, ABC transporters, and thiamine metabolism (Figure 3G and 3H). These findings imply that *B. subtilis* mitigates intracellular U accumulation by enhancing signal perception and efflux capacity. Consistently, U exposure in *Caulobacter crescentus* has been reported to upregulate ABC transporters and related functional categories.[28] The pronounced expression of ABC transporters aligns with their established roles in heavy metal detoxification across various bacteria, typically involving ion sequestration and efflux.[31]

Taken together, the proteomic data indicate that *E. coli* fine-tunes core metabolism at low concentrations of U and maintains this strategy at high concentrations of U stress, whereas *B. subtilis* rapidly activates transport and signaling networks at low concentrations of U, escalating to a comprehensive stress response as the concentration rises. The lower sensing threshold and broader proteomic remodeling observed in *B. subtilis* suggest an investment strategy in anticipatory stress adaptation, which may contribute to its prevalence in metal-contaminated soils.

3.4. Uranium-driven remodeling of antibiotic resistance genes and resistance-associated proteins

Drug efflux pumps play a central role in bacterial survival under antibiotic or metal stress by reducing intracellular toxin concentrations and thereby stabilizing resistance plasmids.[32,33] To determine whether U exposure selects for such pumps, we tracked the abundance of efflux pump transcripts and proteins in both model organisms.

In *E. coli*, all five major pump families were upregulated. Significant increases were observed for ABC transporters (*macA* and *macB*), the multidrug and toxic compound extrusion member *blr*, major facilitator superfamily transporters (*bcr* and *emrY*), resistance–nodulation–division subunits (*acrA*, *acrB*, *mdtA,* and *mdtB*), and small multidrug resistance proteins (*emrE* and *mdtI*). For example, the multidrug and toxic compound extrusion family gene *blr* upregulated with an LFC of 1.28 at 0.05 mg/L U, while *emrY* increased with an LFC of 1.2 at 5 mg/L U (Figure 4A). This upregulation was consistent with metagenomic data from U-impacted soils, where efflux pump genes were also found to be more abundant.[34] In contrast, *B. subtilis* presented the opposite pattern. ABC members (*bmr* and *bmrA*), major facilitator superfamily transporters (*blt* and *lmrB*), and small multidrug resistance pair *ykkCD* were downregulated (Figure 4C). For example, *blt*, which exports macrolides and lincosamides, decreased by an LFC of 1.02 at 0.05 mg/L U and an LFC of 0.57 at 5 mg/L U. Downregulation of these pump systems is expected to reduce the intrinsic antibiotic tolerance of *B. subtilis*, which may explain why this species is less frequently associated with multidrug resistance in metal-contaminated sites.[6,35]

Further proteomic data mirrored the transcriptomic trends. In *E. coli*, 19 resistance-associated proteins were differentially abundant. Among them, AcrA, AcrB, and TolC of the AcrAB–TolC tripartite pump showed LFCs of 0.08 to 0.83 at 0.05 mg/L U (Figure 4B). Induced expression of this pump has been observed in U-challenged *Stenotrophomonas* and *Microbacterium spp*. and is known to accelerate plasmid-borne resistance evolution by maintaining intracellular antibiotic concentrations below the selective threshold.[27,36] In *B. subtilis*, 13 resistance proteins were differentially abundant, including the chromosomal β-lactamase, which were upregulated with LFCs of 0.25 at 0.05 mg/L U and 2.89 at 5 mg/L U (Figure 4D). Thus, although efflux capacity declined, enzymatic detoxification was amplified. Collectively, both model organisms exhibited a net increase in the abundance of resistance-associated proteins, providing proteome-level evidence that U stress promotes the expression and potential acquisition of antibiotic resistance traits.[6] Furthermore, Spearman correlation analysis of all quantified gene–protein pairs revealed a moderate positive correlation between transcriptomic and proteomic profiles in U-stressed strains ($p < 0.05$), indicating concordant expression patterns and dominant transcriptional regulation. Notably, at equivalent U concentrations, *B. subtilis* displayed significantly more discordant pairs than *E. coli* (Table S1), suggesting that transcriptional regulation plays a more predominant role in *B. subtilis* under these conditions.

3.5. Potential pathways of uranium-modulated antibiotic resistance gene expression

3.5.1. Toxin–antitoxin systems

Type II TA systems are critically involved in the evolution of bacterial antibiotic resistance.[37] Under U stress, divergent transcriptional regulation patterns of type II TA systems were observed in *E. coli* and *B. subtilis*. In *E. coli*, six type II TA modules were upregulated, including *mazE/mazF*, *relB/relE*, and *hicB/hicA*. For example, MazF

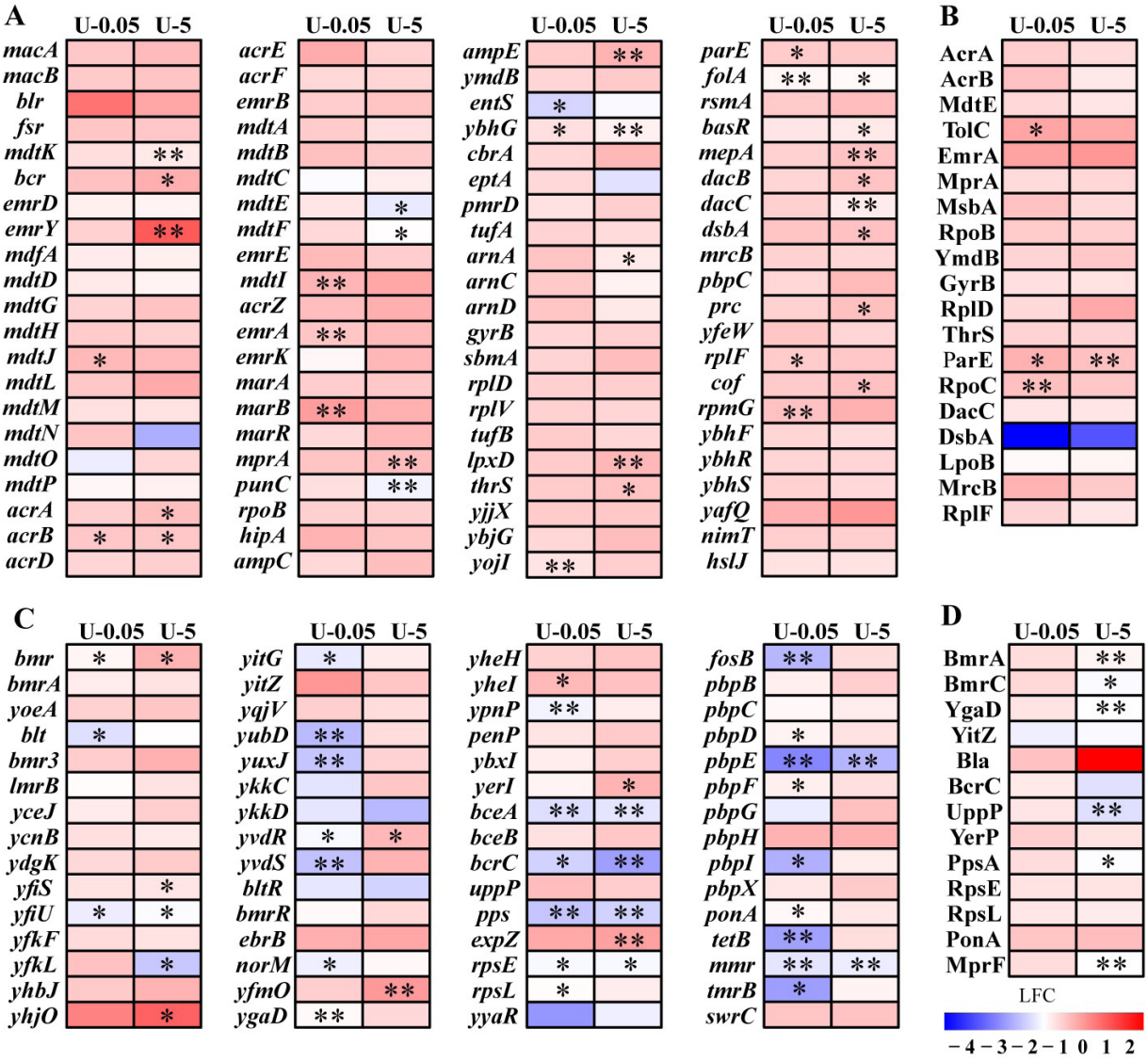

Figure 4. Heatmap of $\log_2$ fold change (LFC) values for differentially expressed ARGs and resistance-associated proteins under uranium (U) stress. (A) *Escherichia coli* gene. (B) *E. coli* protein. (C) *Bacillus subtilis* gene. (D) *B. subtilis* protein. The color gradient represents LFC values (red = upregulation, blue = downregulation), with color intensity positively correlated with the absolute LFC value. *p<0.05 and **p<0.01 indicate significant differences compared to the control group (0 mg/L U). The abbreviations U-0.05 and U-5 refer to 0.05 mg/L U and 5 mg/L U, respectively.

endoribonuclease transcripts showed LFCs ranging from 0.08 to 0.43 (Figure 5A and 5B). A previous study has shown that even moderate *mazF* overexpression can enhance levofloxacin tolerance by cleaving labile mRNAs and slowing growth.[38] Therefore, U stress may remodel metabolic activity and promote adaptation to antibiotics in *E. coli* through activation of TA systems such as *mazE/mazF*. In contrast, *B. subtilis* showed repression of six chromosomal TA loci, including *ndoAI/ndoA* and *spoIISA/spoIISB* (Figure 5C and 5D). The *ndoA* toxin transcript, for instance, decreased with an LFC of 0.67 to 2.04. Paradoxically, reduced *ndoA* expression has been linked to increased resistance to oxidative and antimicrobial stress in *Bacillus*,[37] suggesting that transcriptional downregulation under U stress represents an adaptive strategy rather than a passive response.

3.5.2. Quorum-sensing systems

QS indirectly modulates ARG expression by regulating transcriptional activators and competence development.[39] Under U stress, distinct QS responses were observed in the two species. In *E. coli*, *lsrF*, *lsrG*, and the global regulator

csrA were upregulated with LFCs of 0.37 to 0.94 (Figure 6A). *lsrF* encodes the thiolase that degrades autoinducer-2, thereby resetting population-wide signaling. Concurrently, the general stress sigma factor RpoS increased with LFCs of 0.02 to 0.08 (Figure 6B), reinforcing the previously reported link between QS and stress protection in bacteria exposed to nanoalumina.[40] In contrast, QS genes in *B. subtilis* were generally downregulated under U stress (Figure 6C). Notably, *comA*, the response regulator of the ComQXPA pathway, declined with an LFC of 2.64 at 0.05 mg/L U and 1.62 at 5 mg/L U, respectively. *comA* regulates surfactin synthesis, competence development, and plasmid transfer; its transcriptional repression is therefore expected to reduce horizontal gene flow.[41] Although a slight upregulation of ComA was observed at the protein level (LFCs = 0.04 to 0.14; Figure 6D), the overall transcriptional suppression indicates that this pathway is actively modulated under U stress. Together, these contrasting patterns suggest that *E. coli* fine-tunes QS signals under U stress, whereas *B. subtilis* largely silences the circuit.

3.5.3. Two-component systems

TCS transduce envelope stress into transcriptional responses that include efflux pump and porin genes, thereby influencing antibiotic susceptibility.[42] In *E. coli*, U exposure elevated transcripts of *cpxR–cpxA*, *phoP–phoQ*, and *hprS–hprR* showed LFCs ranging from 0.07 to 0.58 (Figure 7A). A similar role has been reported for the *cpxR–cpxA* system in *Klebsiella pneumoniae*, where it reduces antibiotic susceptibility by repressing porin expression.[43] For *Pseudomonas putida*, the *phoP-phoQ* system confers polymyxin and aminoglycoside resistance via lipid modification and efflux pump activation.[44] The U-induced expression of TCS genes in *E. coli* may therefore produce analogous adaptive effects. Consistent with transcriptional changes, key TCS-associated effector proteins were also upregulated in *E. coli*, including the outer membrane channel TolC (regulated by the CpxR–CpxA system), the response regulator OmpR (controlling the ssrA–ssrB system), and the protease ClpP (part of the SaeR–SaeS regulon). For example, TolC were upregulated with an LFC of 0.63-fold and 0.58 at 0.05 mg/L and 5 mg/L U, respectively (Figure 7B). This coordinated induction suggests a mechanism through which U stress enhances bacterial adaptation by modulating membrane permeability and efflux activity, potentially via systems such as CpxR–CpxA.[45]

B. subtilis responded by upregulating *liaR–liaS*, *degS–degU*, *phoR–phoP*, and *resE–resD* systems at both RNA and protein levels (Figure 7C and 7D). LiaR–LiaS detects cell wall damage caused by vancomycin or bacitracin and triggers protective cell envelope remodeling, whereas DegS–DegU controls antimicrobial peptide production and stress regulons.[46,47] The coordinated induction of these systems indicates that *B. subtilis* fortifies its envelope and activates antibiotic-tolerant phenotypes under U stress, a strategy that complements the earlier repression of efflux pumps.

4. Conclusion

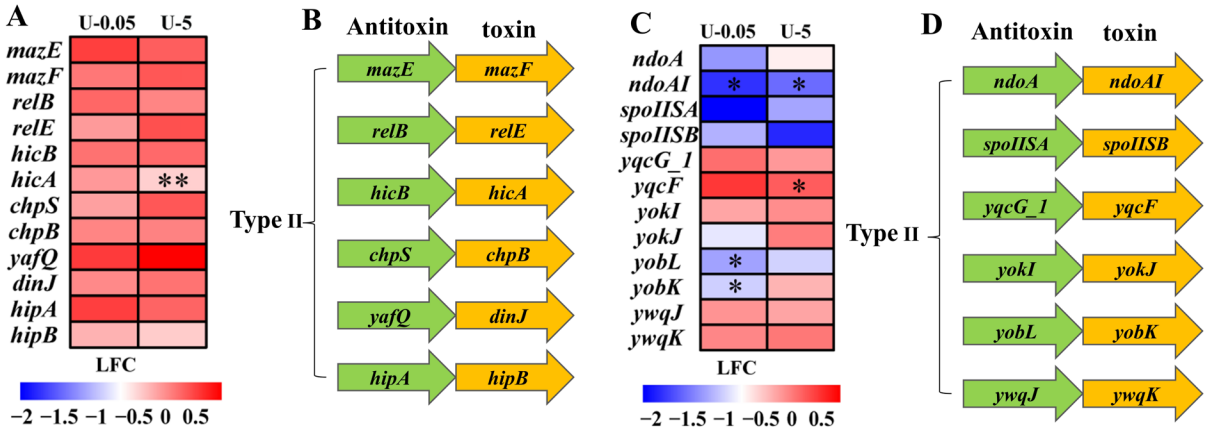

Figure 5. Expression changes of toxin–antitoxin (TA) system-related genes under uranium (U) stress. (A) Heatmap of $\log_2$ fold change (LFC) values for differentially expressed genes in *Escherichia coli*. (B) Genomic organization of TA systems in *E. coli*. (C) Heatmap of LFC values for differentially expressed genes in *Bacillus subtilis*. (D) Genomic organization of TA systems in *B. subtilis*. The color gradient represents LFC values (red = upregulation, blue = downregulation), with color intensity positively correlated with the absolute LFC value. *p<0.05 and **p<0.01 indicate significant differences compared to the control group (0 mg/L U). The abbreviations U-0.05 and U-5 refer to 0.05 mg/L U and 5 mg/L U, respectively.

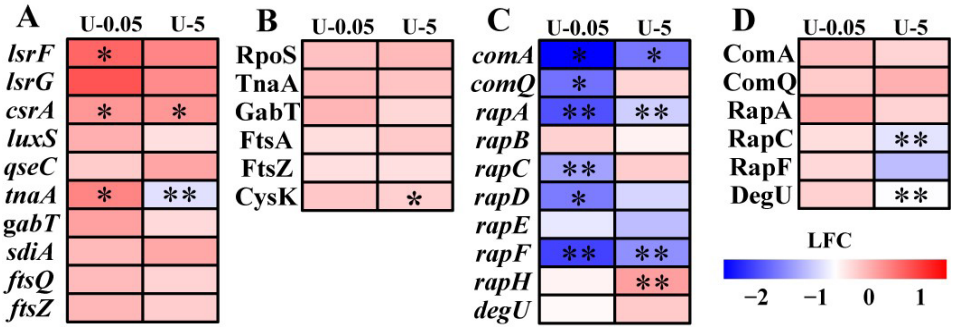

Figure 6. Differential expression of quorum-sensing-associated genes and proteins under uranium (U) stress. (A) *Escherichia coli* gene. (B) *E. coli* protein. (C) *Bacillus subtilis* gene. (D) *B. subtilis* protein. The color gradient represents $\log_2$ fold change (LFC) values (red = upregulation, blue = downregulation), with color intensity positively correlated with the absolute LFC value. *$p < 0.05$ and **$p < 0.01$ indicate significant differences compared to the control group (0 mg/L U). The abbreviations U-0.05 and U-5 refer to 0.05 mg/L U and 5 mg/L U, respectively.

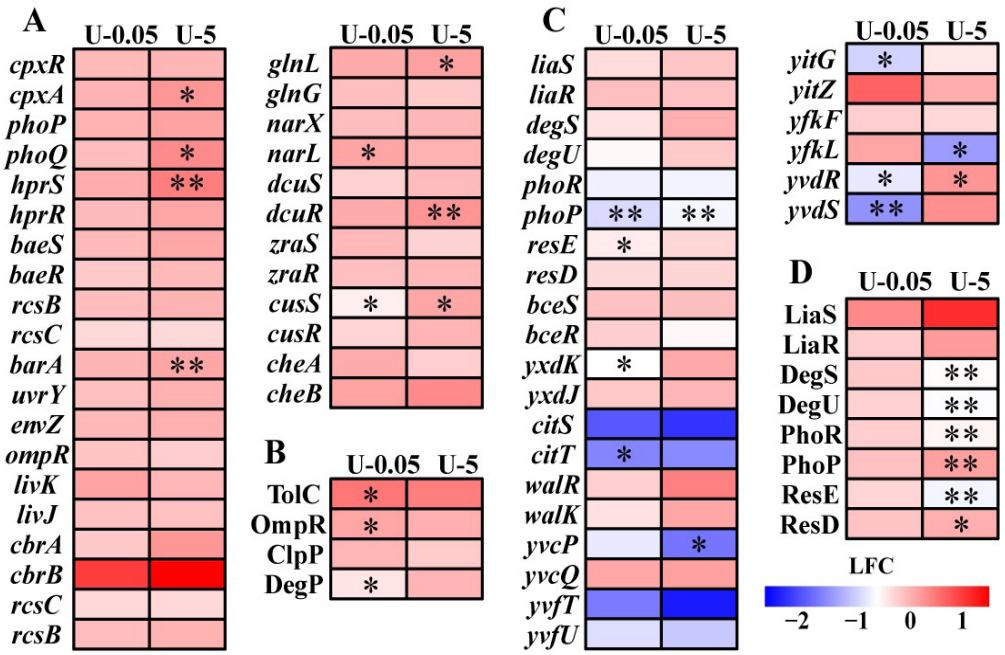

Figure 7. Differential expression of two-component system-related genes and proteins under uranium (U) stress. (A) *Escherichia coli* gene. (B) *E. coli* protein. (C) *Bacillus subtilis* gene. (D) *B. subtilis* protein. The color gradient represents $\log_2$ fold change (LFC) values (red = upregulation, blue = downregulation), with color intensity positively correlated with the absolute LFC value. *$p < 0.05$ and **$p < 0.01$ indicate significant differences compared to the control group (0 mg/L U). The abbreviations U-0.05 and U-5 refer to 0.05 mg/L U and 5 mg/L U, respectively.

In this study, integrated transcriptomics and proteomics revealed two sharply contrasting molecular strategies that enable *E. coli* and *B. subtilis* to withstand U stress at environmentally relevant concentrations. Both species maintained cellular viability, yet their transcriptional profiles were fundamentally divergent. *E. coli* exhibited upregulation of stress and resistance-related genes, whereas *B. subtilis* showed predominant downregulation. Protein-level changes also exhibited clear dose-dependency, with 5 mg/L U inducing substantially stronger shifts than 0.05 mg/L U. *E. coli* activated TA systems, QS circuits, and specific TCS to foster multidrug tolerance. In contrast, *B. subtilis* suppressed these same networks and instead reinforced cell wall-centered TCSs that stiffen envelope integrity. These differential molecular adaptation strategies collectively elucidate the underlying mechanisms by which U drives the development of antibiotic resistance in bacteria. This provides an important theoretical foundation

for assessing the ecological risks of co-contamination with U and bacterial antibiotic resistance. Based on these findings, future work should focus on validating these key regulatory targets in complex environments, quantifying shifts in antibiotic resistance, and verifying the direct functional roles of differentially expressed proteins.

Acknowledgments

None.

Funding

This work was supported by the Natural Science Foundation of Hunan Province, China (No. 2024JJ5329) and the Open Fund of the Key Laboratory of Monitoring for Heavy Metal Pollutants, Ministry of Ecology and Environment (No. KLMHM202523).

Conflict of interest

Chengyun Zhou is the Editor-in-Chief and Shuai Zhou is an Editorial Board Member of this journal, but were not in any way involved in the editorial and peer-review process conducted for this paper, directly or indirectly. Separately, other authors declared that they have no known competing financial interests or personal relationships that could have influenced the work reported in this paper.

Author contributions

Conceptualization: Shuai Zhou, Yuanyuan Gao
Formal analysis: Xiulan Ou
Funding acquisition: Shuai Zhou, Chengyun Zhou
Investigation: Xiulan Ou
Methodology: Jian Song
Resources: Yuanyuan Gao, Chengyun Zhou
Supervision: Yuanyuan Gao, Chengyun Zhou
Visualization: Xiulan Ou, Yi Duan
Writing-original draft: Shuai Zhou, Xiulan Ou
Writing-review & editing: Jian Song, Yi Duan, Shuang Li, Zidong Yang, Yuyu Li, Anqi Chen, Shuying Li, Yuanyuan Gao, Chengyun Zhou

Availability of data

All data generated or analyzed during this study are included in this published article and its supplementary information files.

References

1. Zhang Z, Zhang Q, Wang T, *et al*. Assessment of global health risk of antibiotic resistance genes. *Nat Commun*. 2022;13(1):1553.

   doi: 10.1038/s41467-022-29283-8

2. Khan S, Ahmad K, Farooq M, *et al*. Investigating the teratogenic potential of diclofenac sodium on chick embryos: A warning for pregnant women. *Toxicol Rep*. 2024;12:292-298.

   doi: 10.1016/j.toxrep.2024.02.010

3. Sinegani AAS, Younessi N. Antibiotic resistance of bacteria isolated from heavy metal-polluted soils with different land uses. *J Glob Antimicrob Resist*. 2017;10:247-255.

   doi: 10.1016/j.jgar.2017.05.012

4. Yu S, Wang Y, Shen F, *et al*. Copper-based fungicide copper hydroxide accelerates the evolution of antibiotic resistance via gene mutations in Escherichia coli. *Sci Total Environ*. 2022;815:152885.

   doi: 10.1016/j.scitotenv.2021.152885

5. Islam TN, Meem FS, Yasmin R, *et al*. Co-exposure of chromium or cadmium and a low concentration of amoxicillin are responsible to emerge amoxicillin resistant Staphylococcus aureus. *J Glob Antimicrob Resist*. 2023;35:279-288.

   doi: 10.1016/j.jgar.2023.10.011

6. Zeng X, Cao Y, Wang L, *et al*. Viability and transcriptional responses of multidrug resistant E. coli to chromium stress. *Environ Pollut*. 2023;324:121346.

   doi: 10.1016/j.envpol.2023.121346

7. El Meouche I, Dunlop MJ. Heterogeneity in efflux pump expression predisposes antibiotic-resistant cells to mutation. *Science*. 2018;362(6415):686-690.

   doi: 10.1126/science.aar7981

8. Blanco P, Hernando-Amado S, Reales-Calderon JA, *et al*. Bacterial multidrug efflux pumps: much more than antibiotic resistance determinants. *Microorganisms*. 2016;4(1):14.

   doi: 10.3390/microorganisms4010014

9. Ahmad K, Shah HUR, Qureshi K, *et al*. Arsenic contaminants of groundwater and its mitigation. In: *Soil, Water Pollution and Mitigation Strategies: A Spatial Approach*. Springer; 2024:389.

   doi: 10.1007/978-3-031-63296-9

10. Zhou S, Xiong C, Su Y, *et al*. Antibiotic-resistant bacteria and antibiotic resistance genes in uranium mine: Distribution and influencing factors. *Environ Pollut*. 2022;304:119158.

    doi: 10.1016/j.envpol.2022.119158

11. Zhou S, Huang Z, Song J, *et al*. Metagenomic analysis of the dichotomous role of uranium in regulating intracellular and extracellular antibiotic resistance genes in activated sludge. *Environ Pollut*. 2024;363:125258.

    doi: 10.1016/j.envpol.2024.125258

12. Sun F, Xu Z, Fan L. Response of heavy metal and antibiotic resistance genes and related microorganisms to different

heavy metals in activated sludge. *J Environ Manage*. 2021;300:113754.

doi: 10.1016/j.jenvman.2021.113754

13. Yuan W, She J, Liu J, *et al*. Insight into microbial functional genes' role in geochemical distribution and cycling of uranium: The evidence from covering soils of uranium tailings dam. *J Hazard Mater*. 2024;461:132630.

doi: 10.1016/j.jhazmat.2023.132630

14. Xu N, Qiu D, Zhang Z, *et al*. A global atlas of marine antibiotic resistance genes and their expression. *Water Res*. 2023;244:120488.

doi: 10.1016/j.watres.2023.120488

15. Gao Y, Zhou S, Yang Z, *et al*. Unveiling the role of uranium in enhancing the transformation of antibiotic resistance genes. *J Hazard Mater*. 2024;479:135624.

doi: 10.1016/j.jhazmat.2024.135624

16. Zhou X, Kang F, Qu X, *et al*. Role of extracellular polymeric substances in microbial reduction of arsenate to arsenite by Escherichia coli and Bacillus subtilis. *Environ Sci Technol*. 2020;54(10):6185-6193.

doi: 10.1021/acs.est.0c01186

17. Samuel J, Paul ML, Ravishankar H, *et al*. The differential stress response of adapted chromite mine isolates Bacillus subtilis and Escherichia coli and its impact on bioremediation potential. *Biodegradation*. 2013;24(6):829-842.

doi: 10.1007/s10532-013-9631-8

18. Ma W, Gao B, Guo Y, *et al*. Occurrence and distribution of uranium in a hydrological cycle around a uranium mill tailings pond, Southern China. *Int J Environ Res Public Health*. 2020;17(3):773.

doi: 10.3390/ijerph17030773

19. Wagner SE, Burch JB, Bottai M, *et al*. Groundwater uranium and cancer incidence in South Carolina. *Cancer Causes Control*. 2011;22(1):41-50.

doi: 10.1007/s10552-010-9669-4

20. Pinel-Cabello M, Jroundi F, López-Fernández M, *et al*. Multisystem combined uranium resistance mechanisms and bioremediation potential of Stenotrophomonas bentonitica BII-R7: transcriptomics and microscopic study. *J Hazard Mater*. 2021;403:123858.

doi: 10.1016/j.jhazmat.2020.123858

21. Orellana R, Hixson KK, Murphy S, *et al*. Proteome of Geobacter sulfurreducens in the presence of U (VI). *Microbiology*. 2014;160(12):2607-2617.

doi: 10.1099/mic.0.081398-0

22. Kolhe N, Zinjarde S, Acharya C. Responses exhibited by various microbial groups relevant to uranium exposure. *Biotechnol Adv*. 2018;36(7):1828-1846.

doi: 10.1016/j.biotechadv.2018.07.002

23. Sulaiman JE, Long L, Qian PY, *et al*. Proteomics and transcriptomics uncover key processes for elasnin tolerance in methicillin-resistant Staphylococcus aureus. *mSystems*. 2022;7(1):e01393-21.

doi: 10.1128/msystems.01393-21

24. Wu H, Yu Y, Su Q, *et al*. Combined impact of antibiotics and Cr (VI) on antibiotic resistance, ARGs, and growth of Bacillus sp. SH-1: A functional analysis from gene to protease. *Bioresour Technol*. 2024;414:131579.

doi: 10.1016/j.biortech.2024.131579

25. Khemiri A, Carrière M, Bremond N, *et al*. Escherichia coli response to uranyl exposure at low pH and associated protein regulations. *PLoS One*. 2014;9(2):e89863.

doi: 10.1371/journal.pone.0089863

26. Hufton J, Harding J, Smith T, *et al*. The importance of the bacterial cell wall in uranium (VI) biosorption. *Phys Chem Chem Phys*. 2021;23(2):1566-1576.

doi: 10.1039/D0CP04067C

27. Gallois N, Alpha-Bazin B, Ortet P, *et al*. Proteogenomic insights into uranium tolerance of a Chernobyl's Microbacterium bacterial isolate. *J Proteomics*. 2018;177:148-157.

doi: 10.1016/j.jprot.2017.11.021

28. Yung MC, Ma J, Salemi MR, *et al*. Shotgun proteomic analysis unveils survival and detoxification strategies by Caulobacter crescentus during exposure to uranium, chromium, and cadmium. *J Proteome Res*. 2014;13(4):1833-1847.

doi: 10.1021/pr400880s

29. Lopez D, Vlamakis H, Kolter R. Generation of multiple cell types in Bacillus subtilis. *FEMS Microbiol Rev*. 2009;33(1):152-163.

doi: 10.1111/j.1574-6976.2008.00148.x

30. Jang J, Hur HG, Sadowsky MJ, *et al*. Environmental Escherichia coli: ecology and public health implications—a review. *J Appl Microbiol*. 2017;123(3):570-581.

doi: 10.1111/jam.13468

31. Liu C, Wen L, Cui Y, *et al*. Metal transport proteins and transcription factor networks in plant responses to cadmium stress. *Plant Cell Rep*. 2024;43(10):218.

doi: 10.1007/s00299-024-03310-y

32. Blair JM, Webber MA, Baylay AJ, *et al*. Molecular mechanisms of antibiotic resistance. *Nat Rev Microbiol*. 2015;13(1):42-51.

doi: 10.1038/nrmicro3380

33. Lewis K. Platforms for antibiotic discovery. *Nat Rev Drug Discov*. 2013;12(5):371-387.

doi: 10.1038/nrd3975

34. Jaswal R, Pathak A, Edwards III B, *et al*. Metagenomics-guided survey, isolation, and characterization of uranium resistant microbiota from the Savannah River Site, USA. *Genes*. 2019;10(5):325.

doi: 10.3390/genes10050325

35. Kumar S, Mukherjee MM, Varela MF. Modulation of bacterial multidrug resistance efflux pumps of the major facilitator superfamily. *Int J Bacteriol*. 2013;2013:1-5.

doi: 10.1155/2013/204141

36. Nolivos S, Cayron J, Dedieu A, *et al*. Role of AcrAB-TolC multidrug efflux pump in drug-resistance acquisition by plasmid transfer. *Science*. 2019;364(6442):778-782.

doi: 10.1126/science.aav6390

37. Brantl S, Müller P. Toxin–antitoxin systems in Bacillus subtilis. *Toxins*. 2019;11(5):262.

doi: 10.3390/toxins11050262

38. Zeng X, Hu L, Ai Q, *et al*. Helicobacter macacae MazF interplays with Escherichia coli homologs and enhances antibiotic tolerance. *Helicobacter*. 2023;28(5):e13014.

doi: 10.1111/hel.13014

39. Zhao X, Yu Z, Ding T. Quorum-sensing regulation of antimicrobial resistance in bacteria. *Microorganisms*. 2020;8(3):425.

doi: 10.3390/microorganisms8030425

40. Wang S, Zhao C, Xue B, *et al*. Nanoalumina triggers the antibiotic persistence of Escherichia coli through quorum sensing regulators lrsF and qseB. *J Hazard Mater*. 2022;436:129198.

doi: 10.1016/j.jhazmat.2022.129198

41. Jia R, Wang Y, Wang H, *et al*. The role of quorum sensing effector ComA in regulating biofilm formation and surfactin production in Bacillus subtilis ASAG 010. *Food Biosci*. 2025;69:106842.

doi: 10.1016/j.fbio.2025.106842

42. Bhagirath AY, Li Y, Patidar R, *et al*. Two component regulatory systems and antibiotic resistance in Gram-negative pathogens. *Int J Mol Sci*. 2019;20(7):1781.

doi: 10.3390/ijms20071781

43. Srinivasan VB, Vaidyanathan V, Mondal A, *et al*. Role of the two component signal transduction system CpxAR in conferring cefepime and chloramphenicol resistance in Klebsiella pneumoniae NTUH-K2044. *PLoS One*. 2012;7(4):e33777.

doi: 10.1371/journal.pone.0033777

44. Liu MC, Tsai YL, Huang YW, *et al*. Stenotrophomonas maltophilia PhoP, a two-component response regulator, involved in antimicrobial susceptibilities. *PLoS One*. 2016;11(5):e0153753.

doi: 10.1371/journal.pone.0153753

45. Wang H, Zhang H, Zhang H, *et al*. Outer membrane channel protein TolC regulates Escherichia coli K12 sensitivity to plantaricin BM-1 via the CpxR/CpxA two-component regulatory system. *Probiotics Antimicrob Proteins*. 2021;13(1):238-248.

doi: 10.1007/s12602-020-09671-6

46. Jordan S, Rietkötter E, Strauch MA, *et al*. LiaRS-dependent gene expression is embedded in transition state regulation in Bacillus subtilis. *Microbiology*. 2007;153(8):2530-2540.

doi: 10.1099/mic.0.2007/006817-0

47. Yu C, Qiao J, Ali Q, *et al*. degQ associated with the degS/degU two-component system regulates biofilm formation, antimicrobial metabolite production, and biocontrol activity in Bacillus velezensis DMW1. *Mol Plant Pathol*. 2023;24(12):1510-1521.

doi: 10.1111/mpp.13389